Valence-band splitting in ordered $Ga_{0.5}In_{0.5}P$ studied by temperature-dependent photoluminescence polarization

Takashi Kanata

Department of Applied Science of Material Functions, Division of Science of Materials,
The Graduate School of Science and Technology, Kobe University, Rokkodai, Kobe 657, Japan

Masahiko Nishimoto, Hiroshi Nakayama, and Taneo Nishino

Department of Electrical Engineering, Faculty of Engineering, Kobe University, Rokkodai, Kobe 657, Japan
(Received 10 September 1991)

Valence-band splitting due to symmetry breaking in long-range-ordered $Ga_{0.5}In_{0.5}P$ alloys grown on (001) GaAs by organometallic vapor-phase epitaxy has been systematically investigated with photoluminescence (PL) polarization spectroscopy. PL spectra measured along the [110] and [1$\bar{1}$0] directions showed anisotropy in both the peak energy and intensity together with a significant reduction of the peak energy. It has been found that the anisotropy in polarized PL spectra originates from the valence-band splitting between Γ_{4v}, Γ_{5v}, and Γ_{6v} induced by symmetry breaking due to spontaneous CuPt-type long-range ordering of $Ga_{0.5}In_{0.5}P$. On the basis of theoretical treatments of optical transition rates in the ordered crystal, a general formula describing the relative integrated intensity in PL polarization spectra has been obtained. According to this formula, the valence-band splitting energy has been estimated by measuring the temperature dependence of the polarized PL intensity. The correlations between the anisotropic PL and crystal-growth conditions such as growth temperature and gas-flow ratio in the input column-V and column-III sources are also discussed.

I. INTRODUCTION

There has recently been strong interest in the electronic structure of spontaneously ordered $Ga_xIn_{1-x}P$ alloys grown by organometallic vapor-phase epitaxy (OMVPE) on (001) GaAs substrates. Long-range-ordered $Ga_xIn_{1-x}P$ alloys have the CuPt-type face-centered-cubic (fcc) sublattice constructed by the ordered arrangement of the ($\bar{1}$11) or (1$\bar{1}$1) column-III sublattice plane.[1-8] The long-range ordering (LRO) in the atomic arrangement in OMVPE-grown $Ga_{0.5}In_{0.5}P$ alloys lattice matched to GaAs has been found by transmission-electron-diffraction (TED) observation of the crystalline structure.[1-8] The band-gap energy of these ordered $Ga_{0.5}In_{0.5}P$ alloys strongly depends on the OMVPE growth conditions such as growth temperature and gas-flow ratio in the input column-V and column-III sources, $f(V)/f(III)$.[1,4,7-11]

The band-gap energy determined by electroreflectance (ER) measurements differs by about 50 meV from the normal band-gap energy of disordered alloys, although both alloys have the same composition.[6-8] Extensive measurements, such as photoluminescence (PL) (Refs. 1, 4, 9, and 10) and ER,[6-8] together with TED,[1,4-8] x-ray diffraction,[9] and Raman-scattering spectroscopy,[6] have been performed to clarify the origin of the band-gap reduction (BGR) observed in ordered $Ga_{0.5}In_{0.5}P$. In these experiments, the BGR seems to be closely related to the formation of the ordered region, having CuPt-type column-III sublattices. However, there is no direct evidence of the correlation between the reduction of the band gap and the ordered structure. Problems to be

solved concerning the relation between the BGR and the structural ordering are as follows:[1,4,6-8] (1) The band-gap energy shifts *gradually* with growth temperature and $f(V)/f(III)$ in OMVPE; (2) growth-temperature dependence of the band gap of $Ga_{0.5}In_{0.5}P$ grown at a fixed $f(V)/f(III)$ shows a minimum at around 650 °C, whereas the TED pattern varies from wavy diffraction scattering bands to super-reflection spots $(-\frac{1}{2},\frac{1}{2},\frac{1}{2})$ and $(\frac{1}{2},-\frac{1}{2},\frac{1}{2})$ with the increase of the growth temperature.

Recently, Wei and Zunger performed band-structure calculations of long-range-ordered ternary alloy semiconductors.[11] They made clear the ordering-induced change in the Γ-point electronic structure, such as band-folding relationships and their symmetries for CuAu-I, luzonite, chalcopyrite, famatinite, and CuPt structures of common-anion- and common-cation-type ternary alloys. In particular, the results of the detailed calculations for $Al_{1-x}Ga_xAs$ and $Ga_{1-y}As_ySb$ indicate that the level repulsion between different symmetry states of the binary constituents folding into equal-symmetry states in the ordered ternary structures causes strong variations in the band gaps, e.g., the fundamental band gaps of the ordered ternary alloys are usually smaller than the linear average of the band gaps of the binary constituents. The magnitude of the symmetry-enforced level repulsion strongly depends on the structural deformation and the energy difference between these levels. Moreover, they predicted crystal-field splitting of the valence band of the ordered crystals.

On the other hand, Mascarenhas *et al.* presented anisotropic PL in ordered $Ga_{0.52}In_{0.48}P$ alloys grown on (001) GaAs.[10] They observed PL-peak separations of

several meV between the [110] and [1$\bar{1}$0] polarizations. This result was qualitatively explained as due to the ordering-induced valence-band splitting (VBS) as predicted by Wei and Zunger. However, the peak-separation energy in the polarized PL spectra does not correspond to the VBS energy. In order to verify the ordering-induced changes of the electronic structure, the direct evidence of VBS is necessary together with the precise measurement of BGR.

In this experiment, we have performed systematic studies of anisotropic PL of ordered $Ga_{0.5}In_{0.5}P$ alloys from both viewpoints of experimental approach and theoretical analysis. On the basis of theoretical treatments of optical transitions in a CuPt-type ordered crystal, a general formula about the relative intensity of polarized PL was derived. According to this formula, VBS energy has been estimated by measuring the temperature dependence of polarized PL intensity. We present growth-condition dependences of VBS together with BGR, and discuss LRO with a model based on the CuPt-type $Ga_{0.5+\delta}In_{0.5-\delta}P/Ga_{0.5-\delta}In_{0.5+\delta}P$ ($0 \leq \delta \leq 0.5$) monolayer superlattice (MSL).

II. EXPERIMENTS

The series of $Ga_{0.5}In_{0.5}P$ alloys used in this study were grown on an exact (001) GaAs substrate by using a conventional atmospheric horizontal OMVPE system.[5-8] Triethylgallium, trimethylindium, and phosphine were used as source gases. The growth temperature were varied in the range 600–700 °C. The input gas-flow ratio of $f(V)/f(III)$ ranged from 160 to 1212. Undoped $Ga_{0.5}In_{0.5}P$ epitaxial layers with a thickness of 0.7 μm were grown after the growth of the undoped GaAs buffer layer with the thickness of 0.4 μm. The alloy compositions were determined by measuring precisely the lattice constant perpendicular to the (001) interface plane, $\alpha_\perp$, between $Ga_xIn_{1-x}P$ and GaAs using a double-crystal x-ray diffractometer.[5-8] The epitaxial films were horizontally lattice matched to the GaAs substrate within $\Delta\alpha_\parallel/\alpha_\parallel = \pm 0.1\%$, where $\Delta\alpha_\parallel = |\alpha_\parallel(Ga_{1-x}In_xP)-\alpha_\parallel(GaAs)|$ and $\alpha_\parallel = \alpha_\parallel(GaAs)$. $\alpha_\parallel$ is the horizontal lattice constant. TED observation has been performed for the series of the OMVPE-grown $Ga_{0.5}In_{0.5}P$ alloys.[5,7]

PL spectra were measured in temperatures ranging from 13 to 300 K. The excitation light was the 488-nm line of an Ar-ion laser. The laser-spot area at the sample surface was about 20 mm². We set the polarization of PL along the [110] or [1$\bar{1}$0] crystal axis. The [110] and [1$\bar{1}$0] directions were determined from etch pit anisotropy characteristics. So as to make clear the geometry of the PL polarization measurements, the relationships among the polarization vectors and the ordering directions are depicted in Fig. 1. In this figure, e_x, e_y, and e_z correspond to unit vectors along the [1$\bar{1}$2], [110], and [$\bar{1}$11] directions for the [$\bar{1}$11] ordering, respectively. Similarly, $e_{x'}$, $e_{y'}$, and $e_{z'}$ correspond to those along the [$\bar{1}$12], [1$\bar{1}$0], and [1$\bar{1}$1] directions for the [1$\bar{1}$1] ordering, respectively. $e_{x''}$, $e_{y''}$, and $e_{z''}$ correspond to those along the [100], [010], and [001] directions, respectively. The exciting light polarization was the [110] or [1$\bar{1}$0] direction. The
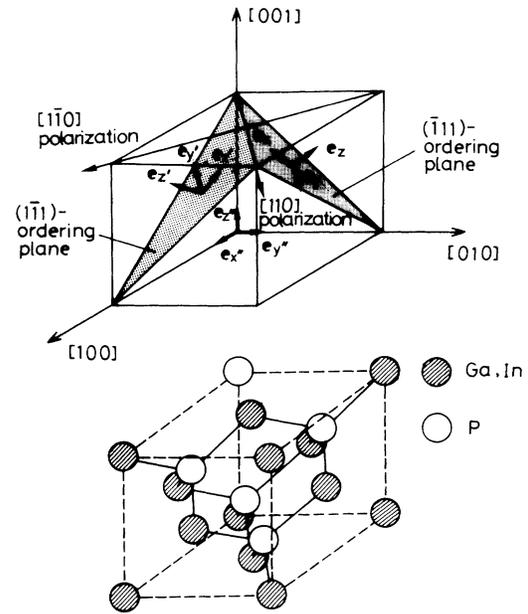

FIG. 1. Relations among polarization vectors and ordering directions.

correction of the obtained data, eliminating a polarization dependence of the optical components, was performed.

III. EXPERIMENTAL RESULTS AND DISCUSSION

A. Photoluminescence polarization spectra

Figures 2(b) and 3 display PL-polarization spectra of $Ga_{0.5}In_{0.5}P$ grown at various growth temperatures and $f(V)/f(III)$, respectively. The spectra were measured at room temperature. As a comparison, a PL spectrum of disordered $Ga_{0.5}In_{0.5}P$ grown by LPE is also shown in Fig. 2(a). The observed PL spectra are independent of the polarized direction of the excitation light. In order to confirm what kind of transitions are the origin of the PL spectra, ER measurements have been performed for these samples.[6-8] The electromodulated reflectance signal, which corresponds to the derivative critical-point structures in the crystal, appears at the same energy position of the PL signal. This implies that the PL corresponds to the band-edge emission.

The PL-polarization spectrum of the disordered alloy in Fig. 2(a) shows the same peak energy and intensity for both polarization directions. The spectra of the OMVPE-grown crystals in Figs. 2(b) and 3, on the other hand, exhibit anisotropy in both the peak energy and intensity. The PL-peak energies of the ordered OMVPE-grown $Ga_{0.5}In_{0.5}P$ are lower than that of the disordered alloy. In the ordered alloys, the PL-peak energy observed in the [110] polarization is slightly lower than that in the [1$\bar{1}$0] polarization. The peak separations are around 10 meV. The PL intensity observed in the [110] polarization is stronger than that in the [1$\bar{1}$0] polarization. To be par-
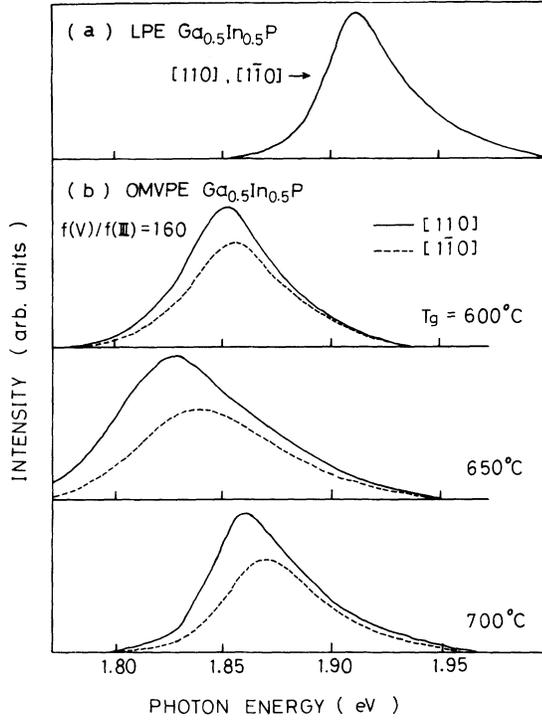
FIG. 2. Polarized PL spectra of (a) disordered (LPE grown) and (b) ordered (OMVPE grown) $Ga_{0.5}In_{0.5}P$ alloys. Polarization was set along the [110] or [1$\bar{1}$0] crystal axis. The ordered alloys were grown at various growth temperatures under a fixed $f(V)/f(III)$ of 160.

FIG. 3. Polarized PL spectra of ordered (OMVPE grown) $Ga_{0.5}In_{0.5}P$ alloys. Polarization was set along the [110] or [1$\bar{1}$0] crystal axis. The ordered alloys were grown at various $f(V)//f(III)$ under a fixed growth temperature of 700 °C.

ticularly noted, a PL signal relating to a disordered structure, which appears around 1.911 eV as shown in Fig. 2(a), is not clearly observed in Figs. 2(b) and 3. In the following analysis and discussion, we neglect the contribution of disordered areas to PL signals.

On the basis of band-structure calculations,[11] the anisotropic PL spectra observed in the ordered samples can be explained by the selection rules for optical transitions derived for the band structure with the rhombohedral symmetry $R\,3m$ instead of $F\bar{4}3m$ of the zinc-blende structure of disordered alloys. The selection rules for electronic-dipole transitions in the band structures can be given by group theory.[12] The results are summarized in Table I, where x, y, and z correspond to allowed polarization components parallel to e_x, e_y, and e_z for the [$\bar{1}$11] LRO, respectively. Similarly x', y', and z' correspond to
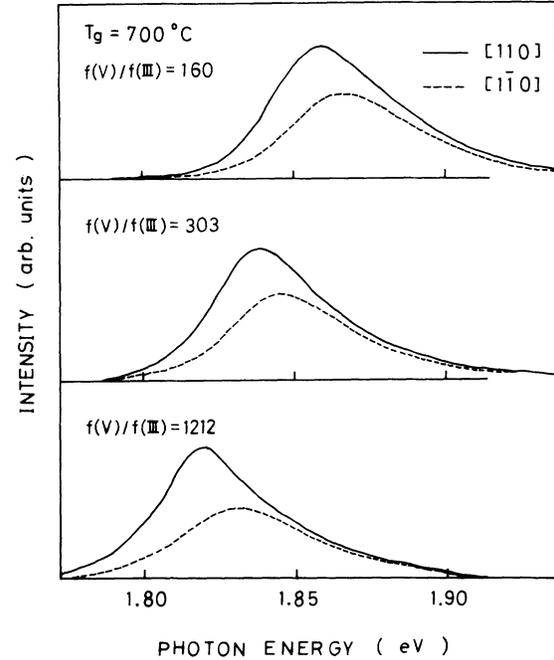
the components parallel to $e_{x'}$, $e_{y'}$, and $e_{z'}$ for the [1$\bar{1}$1] LRO, respectively. x'', y'', and z'' correspond to the components parallel to $e_{x''}$, $e_{y''}$, and $e_{z''}$, respectively.

The Γ_{6c}-Γ_{8v} transition observed in the disordered alloy is isotropic for polarizations along the [110] and [1$\bar{1}$0]. On the other hand, the Γ_{6c}-Γ_{4v},Γ_{5v} transition in the variant of the [$\bar{1}$11] ([1$\bar{1}$1]) ordering has polarization components of x and y (x' and y'), and the Γ_{6c}-Γ_{6v} transition has x, y, and z (x', y', and z'). Thus, the PL-polarization spectrum is given by a mixture of these transitions for both the [110] and [1$\bar{1}$0] polarizations. Here it is noted that the peak separation energy in polarized PL spectra does not correspond to the level splitting between Γ_{6v} and Γ_{4v}, Γ_{5v}.

B. Valence-band splitting due to spontaneous long-range ordering

The effect of VBS could be observed in ER spectra.[6–8] Since the ER signal relating to the Γ_{6c}-Γ_{4v},Γ_{5v} and Γ_{6c}-

TABLE I. Selection rules for electronic-dipole transitions in disordered and ordered $Ga_xIn_{1-x}P$ alloys.

	Symmetry	Representation of CB edge	Representation of VB edge	Allowed polarization
Disordered $Ga_xIn_{1-x}P$	$F\bar{4}3m$	Γ_{6c}	Γ_{8v}	x'',y'',z''
Ordered $Ga_xIn_{1-x}P$	$R\,3m$	Γ_{6c}	Γ_{4v}	x,y,x',y'
			Γ_{5v}	x,y,x',y'
			Γ_{6v}	x,y,z,x',y',z'

Γ_{6v} transitions is complicated, a line-shape fitting is necessary in order to separate the spectrum into constituent signals. However, the fitting by the line-shape function needs many parameters, such as critical-point energy, oscillator strength, strength of the modulated electric field, and its inhomogeneity near the surface of the sample.[13] Such line-shape fitting leads to a difficulty in a unique determination of the splitting energy of the closely located signals. In this experiment, we perform a method for the estimation of VBS energy. This method is based on relative integrated intensities of polarized PL along the [110] and [1$\bar{1}$0] directions.

The relative transition rate T_k with polarization along e_k is given by

$$T_k = \sum_i g_i |(P_k)_{6c,i}|^2 , \qquad (1)$$

where $|(P_k)_{6c,i}|^2$ is a transition probability of the Γ_{6c}-Γ_i transition, and i indicates $4v$, $5v$, or $6v$ for ordering, and $8v$ for disordering. The constant g_i is determined by the degeneracy of the valence bands and population. A relative PL intensity between the polarization along the [110] and [1$\bar{1}$0] directions is $T_y/(T_x/3+2T_z/3)$ for the [$\bar{1}$11] LRO and $T_{y'}/(T_{x'}/3+2T_{z'}/3)$ for the [1$\bar{1}$1] LRO. In the following, we neglect the effect of absorption. We assume that the relative number of photoexcited carriers $N_6/(N_4+N_5)$ is equal to $\exp(-E_v/kT)$, where N_4, N_5, and N_6 are the numbers of carriers at Γ_{4v}, Γ_{5v}, and Γ_{6v}, respectively, E_v is the characteristic energy corresponding to the level splitting in the valence band, and k is the Boltzmann constant. The selection rules for optical transitions listed in Table I and Eq. (1) lead to the following simple formula for the relative PL intensity:

$$S(T) = \frac{3-I_r}{2(I_r-1)} = W_r \exp(-E_v/kT) , \qquad (2)$$

where I_r is $I[110]/I[1\bar{1}0]$, in which $I[110]$ and $I[1\bar{1}0]$

are integrated PL intensities measured along the [110] and [1$\bar{1}$0] directions, respectively, and W_r is a relative transition probability for the Γ_{6c}-Γ_{4v}, Γ_{5v}, and Γ_{6c}-Γ_{6v} transitions. According to this equation, Arrhenius plots of $S(T)$ versus $1/T$ enable us to estimate the activation energy corresponding to the VBS energy.

Figures 4(a) and 4(b) show $S(T)$ as a function of the inverse of temperature for various growth temperatures and $f(V)/f(III)$, respectively. The plots of $S(T)$ show good linear relationships. The splitting energies estimated from the slopes in Fig. 4 are summarized in Figs. 5(a) and 5(b). The estimated VBS energy continuously varies with $f(V)/f(III)$ and growth temperature. The numerical data obtained in our experiment are summarized in Table II. In this table, we also list the Γ_{6c}-Γ_{4v}, Γ_{5v} transition energies and BGR at 13 K, where we take PL-peak energies as the transition energies. Since the peak separation between the PL signals along the [110] and [1$\bar{1}$0] directions gradually decreases with decreasing sample temperature, and the anisotropy in PL-peak energy disappears at below 30 K, the PL spectra measured at below 30 K are caused predominantly by the recombination from Γ_{6c} to Γ_{4v}, Γ_{5v}. It is noted that ratios of BGR to VBS are constant.

Band-structure calculations of a perfectly ordered $Ga_{0.5}In_{0.5}P$ alloy, i.e., a CuPt-type GaP/InP MSL, present a Γ_{6c}-Γ_{4v}, Γ_{5v} transition energy of 1.69 eV at 13 K.[11] This value is far smaller than our obtained data listed in Table II, in spite of the clear observation of VBS and LRO. Furthermore, the variations of BGR and VBS are continuous, as listed in Table II. If the alloy also contains domains of different types of ordering, for example, chalcopyrite and CuAu-I-type orderings, with a smaller bowing coefficient, BGR becomes small.[11] However, this possibility is denied by the observed TED pattern.[5,7] Recent investigation by TEM dark-field images of OMVPE-grown $Ga_{0.5}In_{0.5}P$ reveals that the epitaxial film is occupied by ordered microdomains whose sizes depend
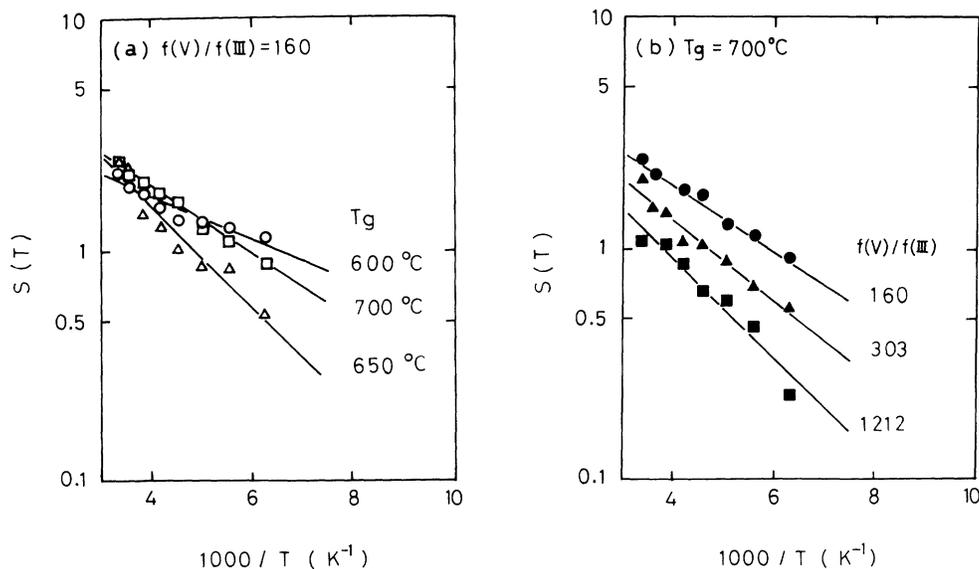

FIG. 4. Plots of $S(T)$ as a function of the inverse of temperature.

TABLE II. Transition, BGR, and VBS energies for OMVPE- and LPE-grown $Ga_{0.5}In_{0.5}P$ alloys.

T_g (°C)	$f(V)/f(III)$	Transition energy[a] (eV)	BGR (meV)	VBS (meV)
OMVPE $Ga_{0.5}In_{0.5}P$		Γ_{6c}-Γ_{4v},Γ_{5v}		
600	160	1.935	52	18.5
650	160	1.888	99	44.3
700	160	1.914	73	28.7
700	303	1.899	88	35.5
700	1212	1.882	105	43.3
LPE $Ga_{0.5}In_{0.5}P$		Γ_{6c}-Γ_{8v}		
		1.987	0	0

[a]Transition energies were measured at 13 K.

on growth temperature and $f(V)/f(III)$,[14] which is similar to results of ordered $Ga_{1-x}As_xP$ alloys reported by Chen, Jaw, and Stringfellow.[15] A domain boundary prevents the propagation of LRO and will weaken influences of LRO in electronic structure. Although this will lead to a weak PL signal related to LRO, it is difficult to consider that the suppression of the effect of LRO causes gradual variation in BGR and VBS. Then we simply consider that most of our experimental data are attributed to LRO in ordered domains.

In order to explain the experimental observation listed in Table II, we propose a CuPt-type LRO structure of $Ga_{0.5+\delta}In_{0.5-\delta}P/Ga_{0.5-\delta}In_{0.5+\delta}P$ ($0 \leq \delta \leq 0.5$) MSL. This MSL structure satisfies the presence of LRO, the observation of VBS, the large transition energy rather than that of the perfectly ordered $Ga_{0.5}In_{0.5}P$ alloy, and its gradual variation by δ. Since we have no information about δ dependence in BGR, we assume that (i) Zunger's

data point for a perfect ordering of $Ga_{0.5}In_{0.5}P$ is quantitatively correct, and (ii) everything varies linearly with δ. According to these assumptions, the Γ_{6c}-Γ_{4v},Γ_{5v} transition energies at 13 K and the VBS are plotted as a function of δ in Fig. 6. The closed and open circles indicate the measured transition energies and VBS, respectively. The closed triangle plots the calculated data by Wei and Zunger for the perfectly ordered $Ga_{0.5}In_{0.5}P$ alloy. The measured transition energies were plotted on the line, and the VBS energies were marked at each δ. The VBS energies also show a linear relationship. Utilizing this figure, the VBS of a perfectly ordered alloy can be estimated. The value is about 115 meV, which is comparable to a VBS energy (230 meV) calculated for a perfectly ordered $GaAs_{0.5}Sb_{0.5}$ alloy with CuPt-type structure.[11]

The relative trend in the TED pattern shows a gradual change from wavy diffraction scattering bands to clear super-reflection spots $(-\frac{1}{2},\frac{1}{2},\frac{1}{2})$ and $(\frac{1}{2},-\frac{1}{2},\frac{1}{2})$ with the
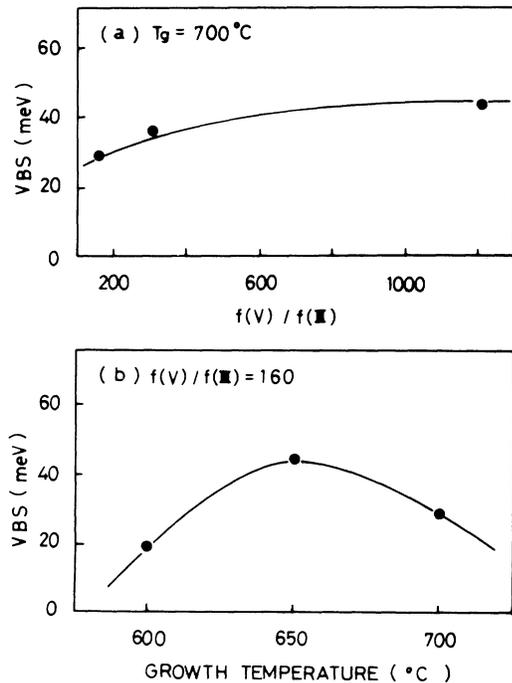

FIG. 5. Growth temperature and $f(V)/f(III)$ dependence of VBS.

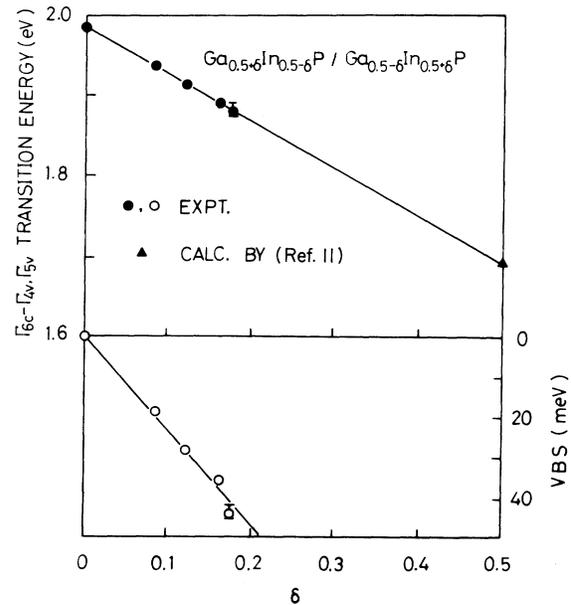FIG. 6. Plots of BGR and VBS as a function of δ in CuPt-type $Ga_{0.5+\delta}In_{0.5-\delta}P/Ga_{0.5-\delta}In_{0.5+\delta}P$ MSL. The closed and open circles indicate the measured Γ_{6c}-Γ_{4v},Γ_{5v} transition energies at 13 K and the VBS energies, respectively. The closed triangle plots the calculated data by Wei and Zunger for a perfectly ordered $Ga_{0.5}In_{0.5}P$ alloy.

increase of growth temperature, whereas the BGR and the VBS show maxima at around 650 °C. Recent Monte Carlo simulations of LRO have pointed out that the diffuse scattering in the electron-diffraction patterns reflects the partial ordering.[16] Then, it seems that a local variation of δ presents itself in the low-temperature-grown samples, and that its variation gradually decreases with increasing growth temperature. Further detailed investigations about the local atomic structure of anions are necessary in order to make clear the relation between the TED pattern and LRO.

IV. CONCLUSIONS

The polarized PL of OMVPE-grown $Ga_{0.5}In_{0.5}P$ alloys grown on exact (001) GaAs has been systematically studied in order to reveal the electronic structure of long-range-ordered $Ga_{0.5}In_{0.5}P$ alloys. On the basis of detailed theoretical analysis of the band structure and the selection rules for optical transitions, it was found that polarized PL spectra of ordered $Ga_xIn_{1-x}P$ alloys show anisotropy originated from VBS induced by symmetry breaking due to LRO. A general formula describing the relative intensity of polarized PL signals has been obtained, and the temperature-dependent PL polarization

reveals VBS energies of ordered $Ga_{0.5}In_{0.5}P$ alloys.

The crystallographic structures of the ordered alloys have been investigated through the anisotropic PL as a function of growth temperature and $f(V)/f(III)$. From our systematic experiment for ordered $Ga_{0.5}In_{0.5}P$ alloys grown at various conditions, it was found that variations of BGR and VBS are continuous and that the BGR-to-VBS ratio is constant. We suggest that a CuPt-type $Ga_{0.5+\delta}In_{0.5-\delta}P/Ga_{0.5-\delta}In_{0.5+\delta}P$ $(0 \leq \delta \leq 0.5)$ MSL is a LRO structure explaining the presence of LRO, the large transition energy, rather than that of the perfectly ordered $Ga_{0.5}In_{0.5}P$, and its continuous variation. Furthermore, local variations of δ seem to explain the change in TED patterns.

ACKNOWLEDGMENTS

[1]A. Gomyo, T. Suzuki, K. Kobayashi, S. Kawata, I. Hino, and T. Yuasa, Appl. Phys. Lett. **50**, 673 (1987).

[2]O. Ueda, M. Takikawa, J. Komeno, and I. Umebu, Jpn. J. Appl. Phys. **26**, L1824 (1987).

[3]P. Bellon, J. P. Chevalier, G. P. Martin, E. Dupont-Nivet, C. Thiebaut, and J. P. Andre, Appl. Phys. Lett. **52**, 567 (1988).

[4]A. Gomyo, T. Suzuki, and S. Iijima, Phys. Rev. Lett. **60**, 2645 (1988).

[5]M. Kondow, H. Kakibayashi, and S. Minagawa, J. Cryst. Growth **88**, 291 (1988); **89**, 614 (1988).

[6]M. Kondow, H. Kakibayashi, S. Minagawa, Y. Inoue, T. Nishino, and Y. Hamakawa, Appl. Phys. Lett. **53**, 2053 (1988).

[7]T. Nishino, J. Cryst. Growth **98**, 44 (1989).

[8]T. Nishino, Y. Inoue, Y. Hamakawa, M. Kondow, and S. Minagawa, Appl. Phys. Lett. **53**, 583 (1988).

[9]S. R. Kurtz, J. M. Olson, and A. Kibbler, Appl. Phys. Lett. **54**, 718 (1989).

[10]A. Mascarenhas, S. R. Kurtz, A. Kibbler, and J. M. Olson, Phys. Rev. Lett. **63**, 2108 (1989).

[11]S. H. Wei and A. Zunger, Phys. Rev. B **39**, 3279 (1989).

[12]G. Burns, *Introduction to Group Theory with Applications* (Academic, New York, 1977).

[13]D. E. Aspnes, in *Handbook of Semiconductors*, edited by T. M. Moss (North-Holland, Amsterdam, 1980).

[14]M. Kondo, H. Kakibayashi, and S. Minagawa (unpublished).

[15]G. S. Chen, D. H. Jaw, and G. S. Stringfellow, J. Appl. Phys. **69**, 4263 (1991).

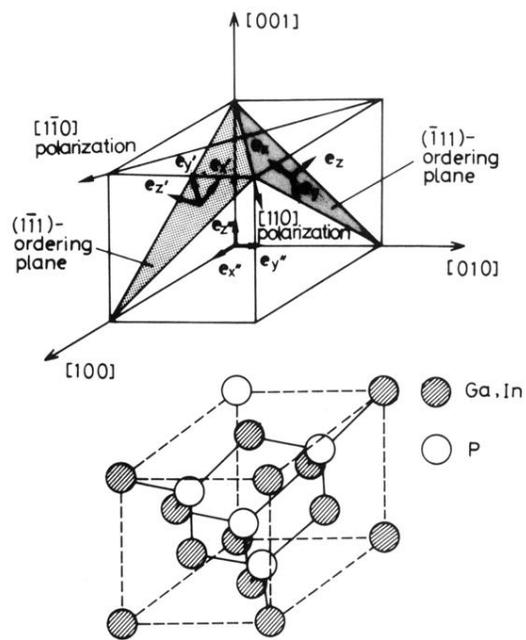[16]S. Matsumura, K. Takano, M. Ishimaru, N. Kuwano, and K. Oki (unpublished).

FIG. 1. Relations among polarization vectors and ordering directions.